MINISTÉRIO DA CIÊNCIA E TECNOLOGIA
INSTITUTO NACIONAL DE PESQUISAS ESPACIAIS

INPE-11283-PRE/6720

THIRD-BODY PERTURBATION USING A SINGLE AVERAGED MODEL

Carlos Renato Huaura Solórzano
Antonio Fernando Bertachini de Almeida Prado

ADVANCES IN SPACE DYNAMICS 4: CELESTIAL MECHANICS AND ASTRONAUTICS,
H. K. Kuga, Editor, 47-56 (2004).
Instituto Nacional de Pesquisas Espaciais – INPE, São José dos Campos, SP, Brazil.
ISBN 85-17-00012-9

INPE
São José dos Campos
2004

ADVANCES IN SPACE DYNAMICS 4: CELESTIAL MECHANICS AND ASTRONAUTICS,
H. K. Kuga, Editor, 47-56 (2004).
Instituto Nacional de Pesquisas Espaciais – INPE, São José dos Campos, SP, Brazil.
ISBN 85-17-00012-9

THIRD-BODY PERTURBATION USING A SINGLE AVERAGED MODEL

Carlos Renato Huaura Solórzano
Antonio Fernando Bertachini de Almeida Prado
National Institute for Space Research (INPE)
São José Dos Campos-SP-12227-010-Brazil
Phone(55-12)3945-6201-Fax(55-12)3945-6226
renato@dem.inpe.br
prado@dem.inpe.br

ABSTRACT

Several papers studied the effect of the third body perturbation in a spacecrafts, usually working with the Hamiltonian of the system or with the disturbing function expressed in an analytic manner. The present paper has the goal of developing a semi-analytical study of the perturbation caused in a spacecraft by a third body with a single averaged model to eliminate the terms due to the short time periodic motion of the spacecraft. Several plots will show the time histories of the Keplerian elements of the orbits involved. One of the most important applications is to calculate the effect of Lunar and Solar perturbations on high-altitude Earth satellites.

INTRODUCTION

The effects of the gravitational attractions of the Sun and the Moon in the orbits of Earth's artificial satellites have been studied in many papers. Kozai [13] writes down Lagrange's planetary equations and the disturbing function due to the Sun or the Moon, including both secular and long periodic terms, but it only gives explicit expressions for the secular terms. Blitzer [8] ignores the specialized techniques of celestial mechanics and it obtains estimates for the perturbations by using methods of classical mechanics. Again, only secular terms are included, and it shows that the principal effect is a precession of the orbital plane around the pole of the ecliptic. Musen [11] shows two systems of formulas for the determination of the long periodic perturbations. The first system uses the theory originally developed by Gauss for a numerical treatment of the very long periodic effects in planetary motion, and the second method is based on the development of the disturbing function in terms of the Legendre polynomials and it finds long periodic terms and the influence on the stability of the orbit.
Cook [5] studied the perturbations due solely by a third body from Lagrange's planetary equations by integrating over one revolution of the satellite. The rates of change of the orbital elements averaged

over one revolution are then written and all first order terms (secular and long-period) are retained in the analysis. The theory is limited to satellites whose semi-major axis does not exceed one tenth of the Moon's distance from the Earth.
After that, Giacaglia [6] obtained the disturbing function for the Moon's perturbations using ecliptic elements for the Moon and equatorial elements for the satellite. Secular, long-period and short-period perturbations are then computed, with the expressions kept in closed form in both inclination and eccentricity of the satellite. Alternative expressions for short-period perturbations of high satellites are also given, assuming small values of the eccentricity.
Hough [10] used the Hamiltonian formed by a combination of the declination and the right ascension of the satellite, the Moon, and the Sun. After that he averaged the Hamiltonian in small and moderate fluctuations and studied periodic perigee motion for orbits near the critical inclinations 63.4^0 and 116.6^0. The theory predicts the existence of larger maximum fluctuations in eccentricity and faster oscillations near stable equilibrium points. Delhaise and Morbidelli [4] investigated the Lunisolar effects of a geosynchronous artificial satellite orbiting near the critical inclination, analyzing each harmonic formed by a combination of the satellite longitude of the node and the Moon's longitude of the node. He demonstrates that the dynamics induced by these harmonics does not show resonance phenomena.
Other researches developed by Broucke [12] and Prado and Costa [1] show general forms of the disturbing function of the third body truncated after the term of second and fourth order, respectively, in the expansion in Legendre polynomials. After that, Costa [7] expanded the order of this model to order eight.

MATHEMATICAL MODELS

Our model can be formulated in a very similar way of the formulation of the planar restricted three-body problem:
- There are three bodies involved in the dynamics: one body with mass $\mathbf{m_0}$ fixed in the origin of the reference system, a second massless body in a three-dimensional orbit around $\mathbf{m_0}$ and a third body in a circular orbit around $\mathbf{m_0}$ (see Figure 1).
- The motion of the spacecraft (the second massless body) is Keplerian and three-dimensional, with its orbital elements perturbed by the third body. The motion of the spacecraft is studied with the single averaged model, where the average is performed with respect to the true anomaly of the spacecraft (**f**). The disturbing function is then expanded in Legendre polynomials.
This section derives the equations used during the simulations. The main body $\mathbf{m_0}$ is fixed in the center of the reference system X-Y. The perturbing body **m'** is in a circular orbit with semi-major axis **a'** and mean motion **n'** ($n'^2 a'^3 = G(m_0 + m')$). The spacecraft is in a three dimensional orbit, with orbital elements: **a**, **e**, **i**, **ω**, **Ω**, and mean motion **n** (where $n^2 a^3 = Gm_0$).
In this situation, the disturbing potential that the spacecraft has from the action of the perturbing body is given by (using the expansion in Legendre polynomials and assuming that r'>>r) (Broucke [12]):

$$R = \frac{\mu' G(m_0 + m')}{\sqrt{r^2 + r'^2 - 2rr'Cos(S)}} = \frac{\mu'(m_0 + m')}{r'} \sum_{n=2}^{\infty} \left(\frac{r}{r'}\right)^n P_n Cos(S) \qquad (1)$$

The parts of the disturbing potential due to P_2 to P_4 are:

$$R_2 = \frac{\mu'}{r'}(\frac{r}{r'})^2 P_2 Cos(S) \quad (2)$$

$$R_3 = \frac{\mu'}{r'}(\frac{r}{r'})^3 P_3 Cos(S) \quad (3)$$

$$R_4 = \frac{\mu'}{r'}(\frac{r}{r'})^4 P_4 Cos(S) \quad (4)$$

The next step is to average those quantities over the short period of the satellite. The definition for average used in this paper is:

$$< G >= \frac{1}{2\pi}\int_0^{2\pi} GdM \quad (5)$$

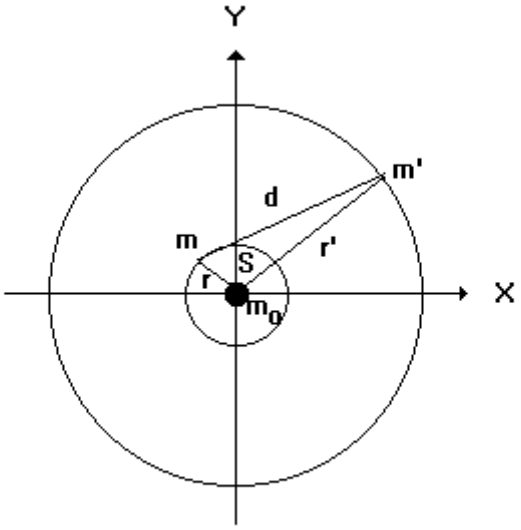

Fig. 1. Illustration of the third body perturbation.

Figure 2 shows the relations between the orthogonal set of vectors $\hat{P}$, $\hat{Q}$, $\hat{R}$ and the orbital plane coordinate system, where $\hat{r}'$ and $\hat{r}$ are unit vectors pointing from the central body to the perturbing body and of central body to the satellite, respectively. M is the mean anomaly of the satellite and M' is the mean anomaly of the perturbing body. The results are for the special case of circular orbits for the perturbing body and with the initial mean anomaly of the perturbing body equal to zero. The following relations are available (Broucke [12]):

$$\alpha = Cos(\omega)Cos(\Omega - M') - Cos(i)Sin(\omega)Sin(\Omega - M') \quad (6)$$

$$\beta = -Sin(\omega)Cos(\Omega - M') - Cos(i)Cos(\omega)Sin(\Omega - M') \quad (7)$$

With those relations it is possible to relate the angle S with the positions of the perturbing and the perturbed bodies.

$$\mathrm{Cos}(S) = \alpha \mathrm{Cos}(f) + \beta \mathrm{Sin}(f) \tag{8}$$

After of process of average the results available are:

$$< R_2 >= \frac{\mu' a^2 n'^2}{2} (\frac{a'}{r'})^3 ((1 + \frac{3}{2} e^2)(\frac{3}{2}(\alpha^2 + \beta^2) - 1) + \frac{15}{4} e^2 (\alpha^2 - \beta^2)) \tag{9}$$

$$< R_3 >= \frac{\mu' (a)^3 (n')^2}{2a'} (\frac{a'}{r'})^4 [\frac{15\alpha e(4 + 3e^2)}{8} - \frac{25\alpha^3 e(3 + 4e^2)}{8} + \frac{75\beta^2 (e^2 - 1)\alpha e}{8}] \tag{10}$$

$$\begin{aligned} < R_4 >= {} & \frac{3\mu' (a')^3 (a)^4 (n')^2}{64 (r')^5} ((8 + 40(e)^2) + 15(e)^4) - 10\alpha^2 (4 + 41(e)^2 + 18(e)^4) \\ & + 35\alpha^4 (1 + 12(e)^2 + 8(e)^4) - 10\beta^2 (4 - (e)^2 - 3(e)^4) + 70\alpha^2 \beta^2 (1 + 5(e)^2 - 6(e)^4) \\ & + 35\beta^4 ((e)^2 - 1)^2) \end{aligned} \tag{11}$$

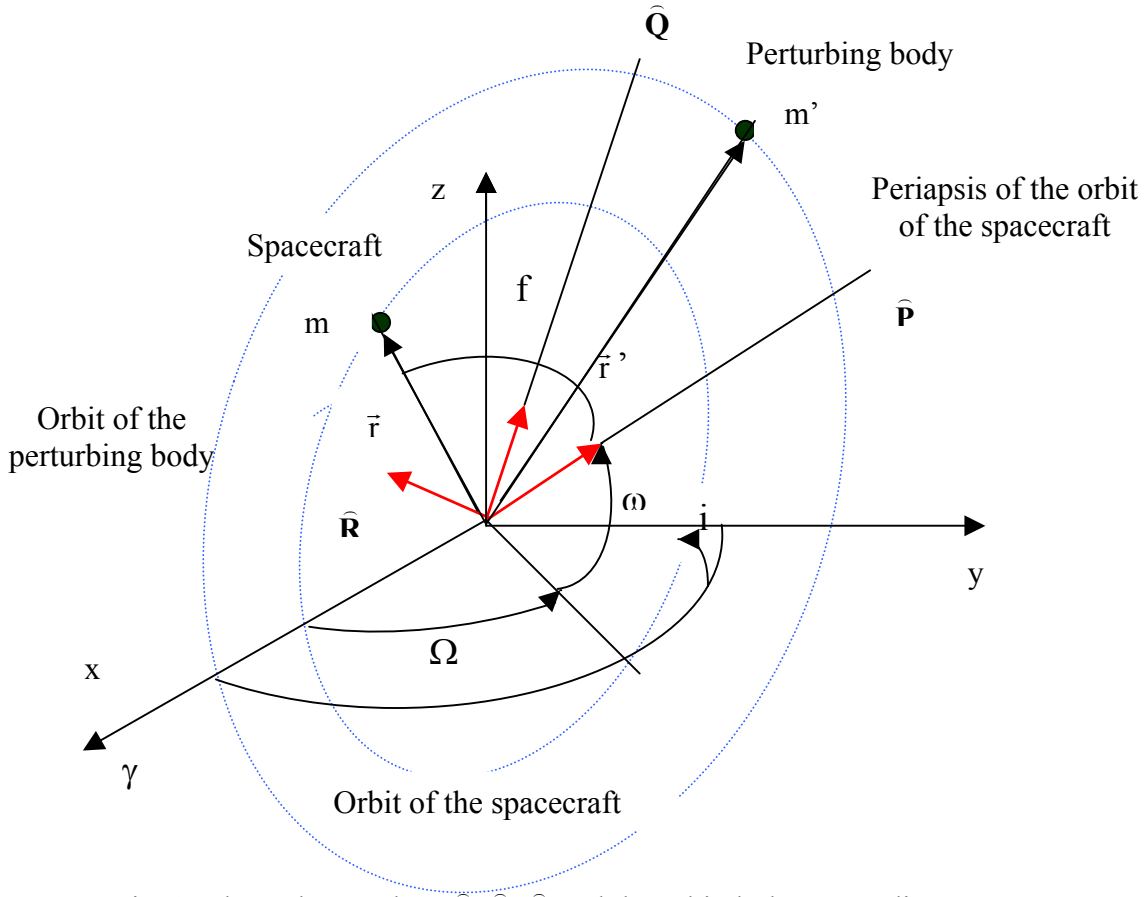

Fig. 2. The orthogonal set $\hat{\mathbf{P}}$, $\hat{\mathbf{Q}}$, $\hat{\mathbf{R}}$ and the orbital plane coordinate system.

The next step is to obtain the equations of motion of the spacecraft. From the Lagrange's planetary equations, that depends on the derivatives of the disturbing function (see Taff [9]). It is noticed that

the semi-major axis always remains constant. This occurs because, after the averaging, the disturbing function does not depend on Mo:

RESULTS

Looking for the behavior of the orbital elements for values of the initial inclination above and below the critical value, it is visible that the inclination oscillates with a varied amplitude. The so called "critical angle of the third-body perturbation" is a value for the inclination between the orbital planes of the perturbing and the perturbed bodies, such that any near-circular orbit with inclination below this remains near-circular.

From the evolution of the inclination for a initial value of 20 deg, it is clear that the amplitude of the variation is of the order of 0.0007 (see Figure 3). Figure 4 shows the evolution of the inclination for a initial value of 35 deg, that is a value near critical (39.231 deg). It is possible to identify a periodic behavior with an amplitude of 0.0011. It is also visible that for the case showed in Figure 3 the oscillations occur around a line of constant inclination and in Fig. 4 these oscillations occur around a line that also has a sinusoidal shape. The results available in the literature regarding the double averaged problem confirm and explain this behavior (Prado [2]).

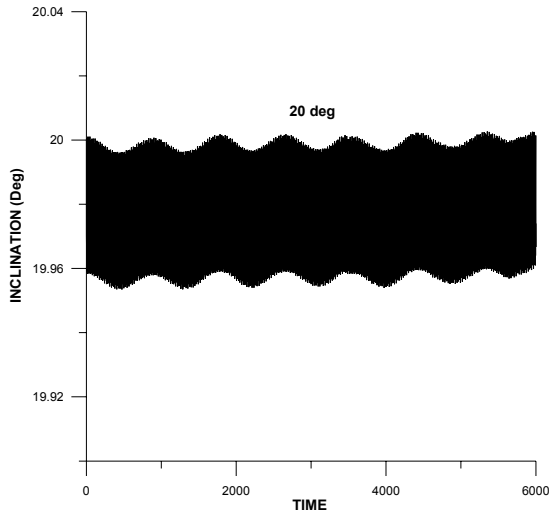

Fig. 3. Plots of the Inclination for i(0) = 20 deg

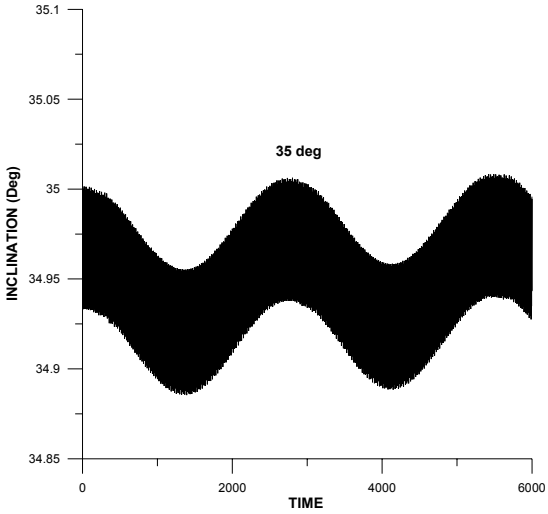

Fig. 4. Plots of Inclination for i(0) = 35 deg

For the cases of initial inclinations above the critical value, the inclination starts at the initial value, decreases to the critical value and then it returns again to its original value (see Figures 5 and 6).

The results are very similar to the ones obtained with the double averaged approach (Prado [2]). The reason for that is the scale used in the plots. The difference between both methods is the existence of a short period oscillation around the main lines giving by the double averaged method and this oscillation is not visible in the scale used in the plots.

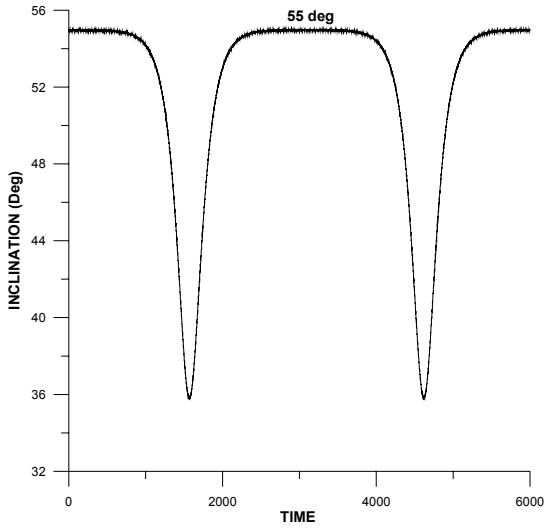

Fig. 5. Plots of Inclination for i(0) = 55 deg

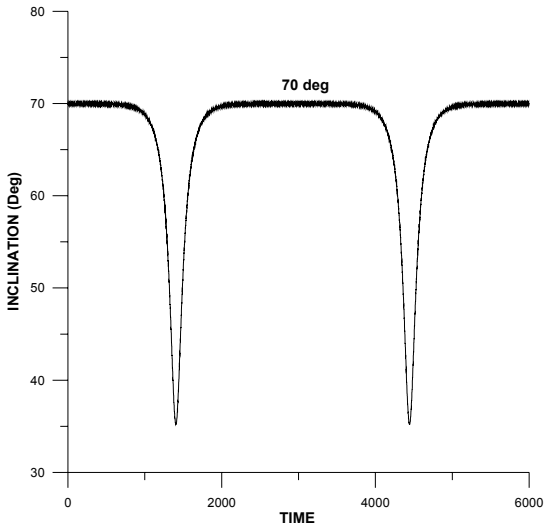

Fig. 6. Plots of Inclination for i(0) = 70 deg

The next simulations show results for initial inclinations below the critical value. The scales of the plots has to be noticed, and they show that the evolution of the inclination can be expressed in straight line (see Figure 7).

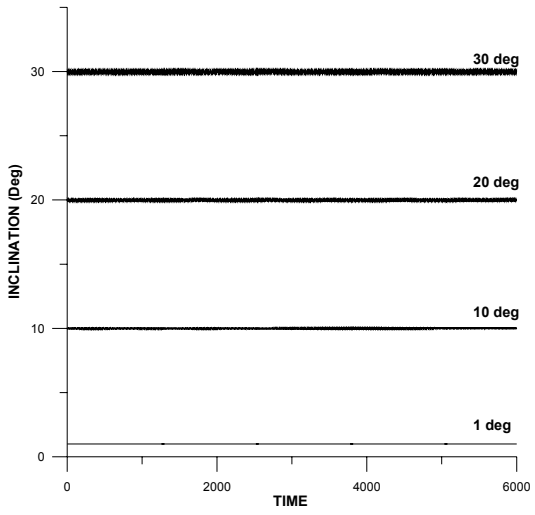

Fig. 7. Plots of Inclination for i(0) < i critical

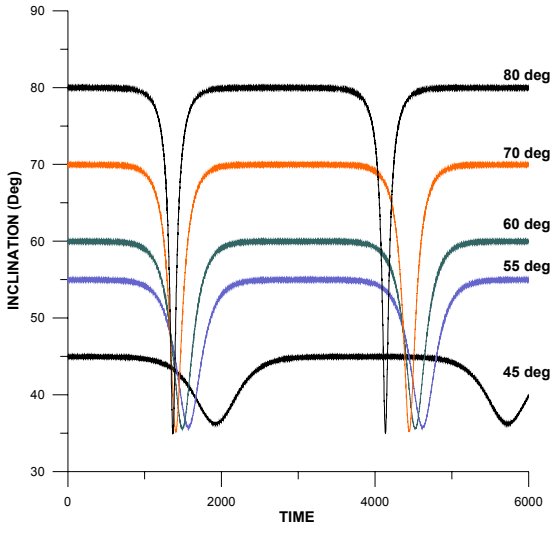

Fig. 8. Plots of Inclination for i(0) > i critical

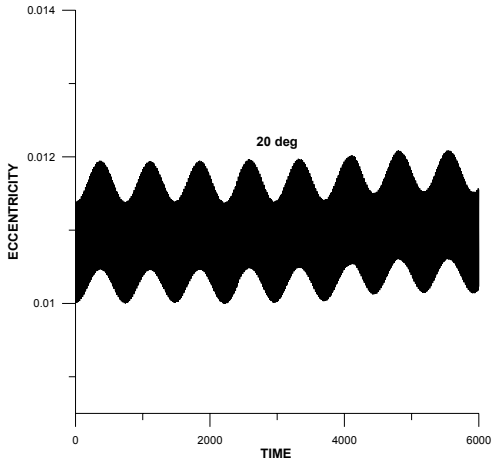

Fig. 9. Plots of the Eccentricity for i(0) = 20 deg

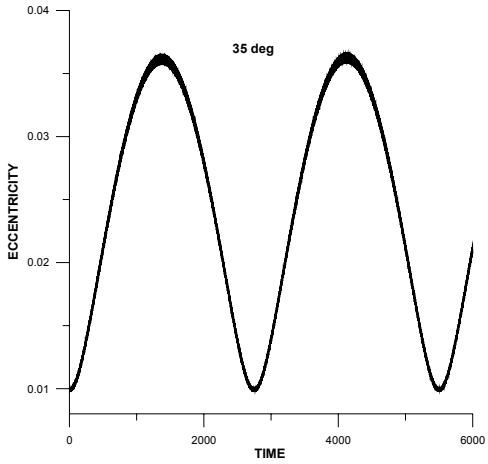

Fig. 10. Plots of the Eccentricity for i(0) = 35 deg

The evolutions of the inclination for starting values above the critical inclination show curves that has the characteristic behavior of starting with an initial value, decreasing to the critical value, then returning to its original value (see Figure 8). Now, we measure the effect of increasing the initial inclination. The results show that the time for reaching the critical value is reduced. The next step is to study the evolutions of the eccentricity. It oscillates with a very small amplitude for values of the initial inclination below critical (see Figure 9). The oscillation have an amplitude of 0.003 for the initial inclination of 20 deg. Figure 10 shows the evolution of the eccentricity for values of the initial inclination near the critical value, and it is possible to identify the evolutions with amplitude of 0.025.

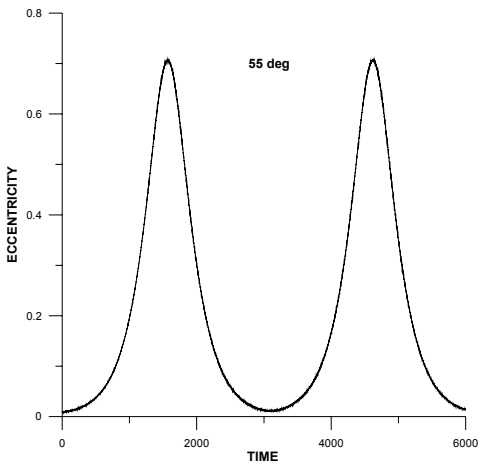

Fig. 11. Plots of the Eccentricity for i(0) = 55 deg

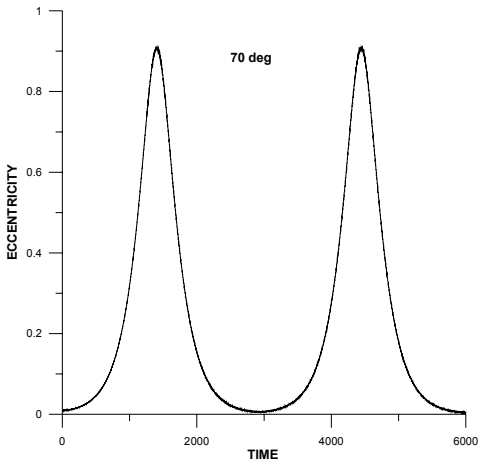

Fig. 12. Plots of the Eccentricity for i(0) = 70 deg

It is important to notice that, when the eccentricity reach its maximum amplitude, the inclination reach its smaller amplitude for the case of initial inclination near or above of critical value (see the Figures 4, 5, 6, 10, 11, 12).

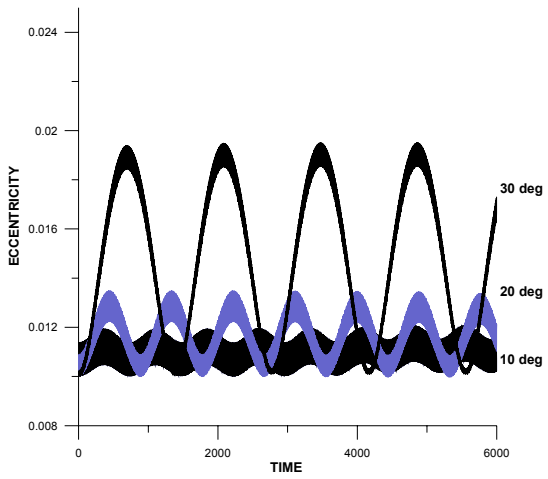

Figure. 13. Plots of the Eccentricity for i(0) < i critical

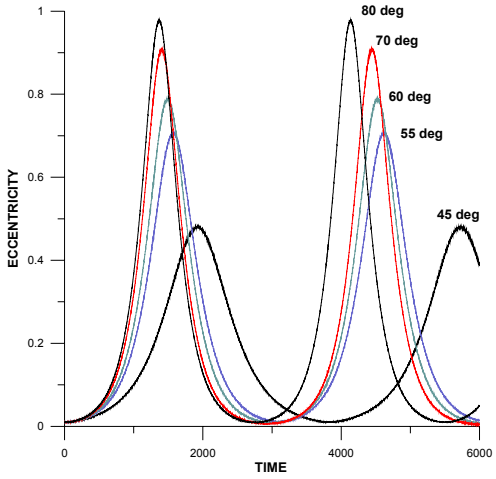

Fig. 14. Plots of the Eccentricity for i(0) > i critical

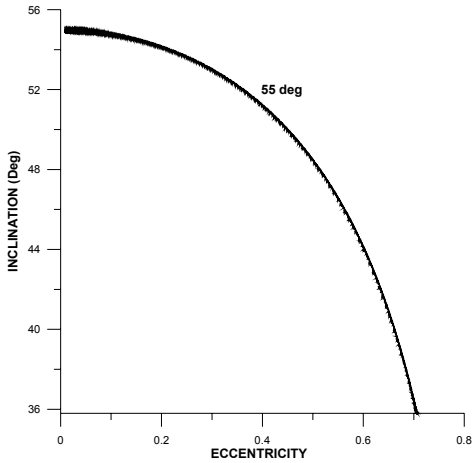

Fig. 15. Eccentricity vs. Inclination for i (0) = 55 deg.

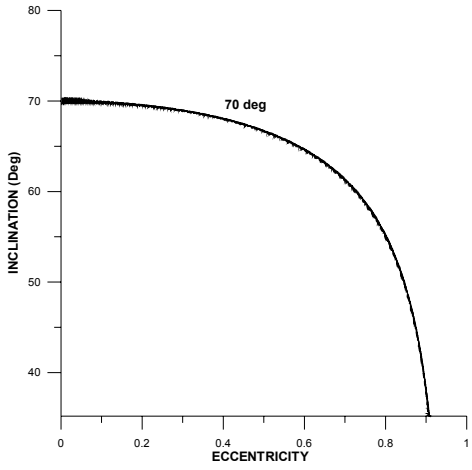

Fig. 16. Eccentricity vs. Inclination for i (0) = 70 deg.

When plots of the eccentricity for values of the initial inclination below critical (see Figure 13) are made, they show that the amplitudes decrease. This is important to keep the stability of the orbits. Figure 14 shows the evolutions of the eccentricity for values of the initial inclination above the critical value.

Figures 15 and 16 have a characteristic behavior. In these simulations it is shown the plots for initial inclination above the critical value. It is possible to identify the evolution of the inclination vs. the eccentricity, to notice that, when the inclination reaches it maximum value, the eccentricity reaches its minimum value. This curves is periodic for the evolution of the inclination and eccentricity. The orbital elements used for those simulation are: a[0]=0.341, e[0]=0.01, $\Omega[0]=0$, $\omega[0]=0$. Remember that the time is defined such that the period of the disturbing body is 2π (canonical system of units).

CONCLUSIONS

This paper develops the third body perturbation using a single averaged model, expanding the perturbation function up to the fourth order. The results show the behavior of the orbits with respect to the initial inclination. The orbital elements present small oscillations and/or secular behavior. This semi-analytical model is able to study the evolutions of the orbital elements and the importance of the critical inclination in the stability of near circular orbits. The results are compared with the ones obtained by the double-averaged model. It confirms the same properties obtained from this model. The main difference in the results is the existence of oscillations around a main line given by the double-averaged model. Several plots will show the time histories of the Keplerian elements of the disturbing function of the third body truncated after the term of fourth and eight order given by singular averaged model is development by Solórzano[3].

REFERENCES

[1] A.F.B.A Prado, I.V. Costa, “Third Body Perturbation in Spacecraft Trajectory,” IAF Paper 98-A.4.05, 49th International Astronautical Congress, Melbourne, Australia, Sept.-Oct, 1998.

[2] A.F.B.A Prado, “Third-Body Perturbation in orbits around natural satellites”, To be published in the Journal of Guidance, Control and Dynamics, 2002.

[3] C.R.H. Solórzano, “Third-Body perturbation using a single averaged model”, Master Dissertation, National Institute for Space Research (INPE) 2002, São José dos Campos, SP, Brazil.

[4] F. Delhaise, A Morbidelli, “Luni-solar effects of Geosynchronous orbits at the critical inclination,” Celestial Mechanics and Dynamical Astronomy, V. 57, pp. 155-173, 1993.

[5] G.E. Cook, "Luni-solar perturbations of the orbit of an earth satellite,” The Geophysical Journal of the Royal Astronomical Society, V. 6, No 3, pp. 271–291, April 1962.

[6] G.E.O. Giacaglia, "Lunar perturbations on artificial satellites of the earth," Smithsonian Astrophysical Observatory, Special Report 352, October 1973.

[7] I.V. Costa, “Study of the Third-Body Perturbation in a Earth’s Artificial Satellite,” Master Dissertation, National Institute for Space Research (INPE), São José dos Campos, SP, Brazil.

[8] L. Blitzer, "Lunar- Solar perturbations of earth satellite," American Journal of Physics, V. 27, pp. 634-645, 1959.

[9] L.G Taff, “Celestial Mechanics,” A Wiley – Interscience Publication, pp.308-309, 1985

[10] M.E. Hough, "Lunisolar perturbations," Celestial Mechanics and Dynamical Astronomy, V.25, pp. 111-136, 1981.

[11] P. Musen, “On the Long-Period Lunar and Solar Effect on the Motion of an Artificial Satellite,” Journal of Geophysical Research, V. 66, pp. 2797-2813, 1961.

[12] R. A. Broucke, "The Double Averaging of the Third Body Perturbations"; Classnotes, Texas University, Austin-TX-USA, 1992.
[13] Y. Kozai, "On the Effects of the Sun and Moon Upon the Motion of a Close Earth Satellite," Smithsonian Inst. Astrophysical Observatory, Special Report 52, March 1959.